

FAULT SLIP RATES IN ARMENIA BY THE GPS DATA

© 2006 г. V. Davtyan*, E. Doerflinger**, A. Karakhanyan*,
H. Philip**, A. Avagyan*, C. Champollion**, and R. Aslanyan***

*GEORISK Scientific Research Company, 24a Marshal Baghramyan avenue,
375019, Yerevan, Armenia, e-mail: georisk@sci.cm

**Lithosphere Dynamics Laboratory, Montpellier-2 University, Place E. Bataillon
34095 Montpellier cedex 05, France, e-mail: Herve.Philip@dstu.univ-montp2.fr

***Institute of Geological Sciences, National Academy of Sciences of Armenia,
24a Marshal Baghramyan avenue, 375019, Yerevan, Armenia

Submitted to the editors on 20.03.2006

Since 1998, Montpellier-2 University (France), GEORISK Scientific Research CJS and Institute of Geology of the National Academy of Sciences (Armenia) launched GPS measurements to investigate deformations in the active fault zones. The analysis of the obtained deformation rates allowed rejection of the existence of rigid, non-deformed lithosphere blocks in central and northern Armenia suggested by Balassanian et al. (1999 a, b). The conducted GPS studies enabled estimation of deformation rates in fault, or fault segment zones in central and northern Armenia.

Introduction

Armenia and the neighboring regions of Azerbaijan, Georgia and Eastern Turkey are located in the central part of the zone of continental collision of the Arabian lithosphere plate. These areas undergo N-S shortening and E-W extension accompanied by faulting and earthquakes (Jackson and McKenzie, 1984; Dewey et al., 1986; Taymaz et al., 1991). This convergence estimated at 25 mm/y by NUVEL – 1A (DeMets et al., 1990) and 18±2 mm/y by GPS data (McClusky et al., 2000) has moved the Anatolian block to the west, and the Iranian block to the east.

The North-Anatolian, East-Anatolian, Zagros, Alborz and other active faults on the flanks of the Arabian collision zone define the blocks of Anatolia and Iran. These faults are each from 700 km to 1700 km long and are characterized by horizontal slip rates of 7 to 30 mm/yr (Ambraseys and Jackson, 1998). Numerous strong earthquakes ($M=7.5-7.7$) have been associated with these faults (Jackson and McKenzie, 1988, Ambraseys and Melville, 1982, Ambraseys and Jackson, 1998, Reilinger and Barka, 1997).

Shorter strike-slip faults with reverse or normal slip components are predominant in Armenia. Each of these faults is not more than 350–450 km long, in the meantime, earthquakes of $M=7.2-7.5$ are nevertheless associated with these faults (Ambraseys and Melville, 1982; Berberian, 1997; Karakhanyan et al., 2004). Manifestations of geodynamic and seismic activity in the region are complex and have not been understood completely. The available estimates of slip rates for these faults, and of maximum possible earthquake magnitudes and earthquake recurrence periods are fragmentary and not finely clear.

The GPS data indicate that deformations resulting from the Arabian-Eurasian plate convergence are partitioned between right-lateral strike-slip faulting in eastern Turkey and thrusts along the front of the Caucasus (Barka and Reilinger, 1997, McClusky et al., 2000). Reilinger and Barka (1997) suggest that the Caucasus region can be better described from the standpoint of distributed deformation, rather than by rigid block motions. The total shortening across the Lesser and Greater Caucasus by the data of Reilinger and Barka (1997) and McClusky et al (2000) has a rate of 10±2 mm/y, and ~

60% of this shortening is accommodated within the Greater Caucasus.

Based on the GPS data, Guseva et al (1998) and Shevchenko et al (1999) make a counter assumption that the deformations caused by the northern drift of the Arabian Plate are completely absorbed by the ophiolitic belts of Northern Anatolia and the Lesser Caucasus, to a considerable extent in Armenia, and are not transferred farther northerly, to the Greater Caucasus.

Such contradictions between the interpretations can be ascribed to the lack of source GPS data obtained from an insufficiently dense network of observation points and within rather short period of observations. Moreover, the differences between the listed interpretations can result from use of different geodynamic models. It is noteworthy, that interpretations by Barka and Reilinger (1997), McClusky et al., (2000), likewise those suggested by Guseva et al (1998) and Shevchenko et al (1999), almost did not take into account the geometry, kinematics and slip rates of individual active faults derived by geological and GPS evidence.

The recent years' geology studies in Armenia allowed identification of the systems of active strike-slip faults with slip rates estimated at 0.5 mm/y (Philip et al., 2001; Avagyan, 2001) to 4 mm/y (Trifonov et al. 1990; Trifonov et al., 1994; Karakhanyan et al. 2004). In Armenia, the active strike-slip and reverse faults form a structural arc that bends to the north (Fig.1). Deformation within the arc is characterized by E-W-oriented reverse faults and thrusts, oblique strike-slip faults, and N-S-oriented normal faults. The outer part of the arc is limited by the two active faults – Zheltorechensk-Sarighamish (ESF) and Pambak-Sevan-Syunik (PSSF). The Zheltorechensk-Sarighamish fault is a left-lateral strike-slip fault, while the Pambak-Sevan-Syunik is a right-lateral strike-slip fault. The inner part of the arc is delimited by the left-lateral strike-slip Akhouryan Fault (AF) and the right-lateral strike-slip Garni Fault (GF).

The best-studied are the PSSF and the GF. The kinematics of these faults is estimated as strike-slip with a vertical component of varying sense, but mostly it is reverse-slip (Trifonov et al., 1994; Philip et al., 2001; Karakhanyan et al., 1997a, 1997b, 2004; Avagyan, 2001). The greatest vertical co-seismic displacement is measured as 3.6 m for the PSSF and 1.8 m for the GF. The long-term horizontal displacement estimated by

morphology data comprises 2000 ± 250 m for the PSSF and 300 ± 50 m for the GF (Trifonov et al., 1994, Philip et al., 2001). The geological data allow estimation of the horizontal slip rate as $3\text{--}4 \text{ mm/y}$ for the PSSF (Trifonov et al., 1990) and $3\pm0.5 \text{ mm/y}$ for the GF (Trifonov et al., 1994).

Since 1991, recent rates of lithosphere deformation have been studied in Armenia by means of GPS measurements (Reilinger et al., 1996; Reilinger, Barka, 1997; McNlusky et al., 2000). The permanent NSSP station installed in Yerevan and included in the Mediterranean GPS Network (MGN) has been operative in Armenia since 1996. The MGN network was deployed to study global deformations in the zone of continental plate collision, and to estimate slip rates and rotation poles of lithosphere plates and blocks.

In 1998, Montpellier-2 University (France), GEORISK Scientific Research CJS and Institute of Geology of the National Academy of Sciences of the RA (Armenia) launched GPS measurements to investigate deformations in the active fault zones. For this purpose, a GPS network of 22 points was deployed in the northern and central parts of Armenia in addition to the MGN network (Doerflinger et al., 1999). In this article, we present the results of 3 sessions of measurements conducted within this network from 1998 to 2003.

The geometry of the GPS network

The net of GPS observations, consisting of 22 points, was installed in September 1998. The layout of the network is shown in Fig.1.

In designing network geometry, the principle we applied was to cross the main active faults of Armenia (PSSF, GF, AhF, ESF, and other) with at least 2 or 3 profiles of GPS measurement points. In each of such

profiles, 2 points were installed at a close distance from the fault (2 to 7 km on both sides) and the other 2 to 4 points were positioned at a greater distance of 15-70 km (Fig.1).

Such geometry of the network was expected to enable control of displacements in large fault zones, and to identify any potential contribution to the total displacement from unaccounted minor faults and inelastic deformation within the fault-delimited areas.

The network was deployed so that to include areas of interest for their geodynamics in the north and in the center of Armenia, the most active ones and posing the highest seismic risk. The net covered an area of 150 km latitudinal and 180 km longitudinal strike. Conditionally, it can be subdivided into the three areas:

1. The central part of the North-Armenian Active Fault Arc represents an area of convergence of the most active faults, including the PSSF, GF, AF, and ESF (Fig.1). The geodynamics in the upper North-Armenian Arc is of interest considering that this is a place of crossing between two right-lateral and the other two left-lateral strike-slip faults combined with a complex pattern of shortening and squeezing deformations inside the areas delimited by the faults. Besides, a geodynamic interpretation is required for the extension zone of the Javakhk Highland that has accommodated a young volcanism area in front of the arc tip, and numerous weak earthquakes (Fig.1). The social importance of the studied area is related to the cities of Gyumri and Vanadzor (the second and the third largest cities in Armenia, respectively) characterized by high rate of seismic risk. The Spitak earthquake of 1988 ($M=7.0$) associated with the activation of GF, PSSF and ESF faults in this area, destroyed the cities of Gyumri, Vanadzor and many villages around, and killed more than 25,000 people.

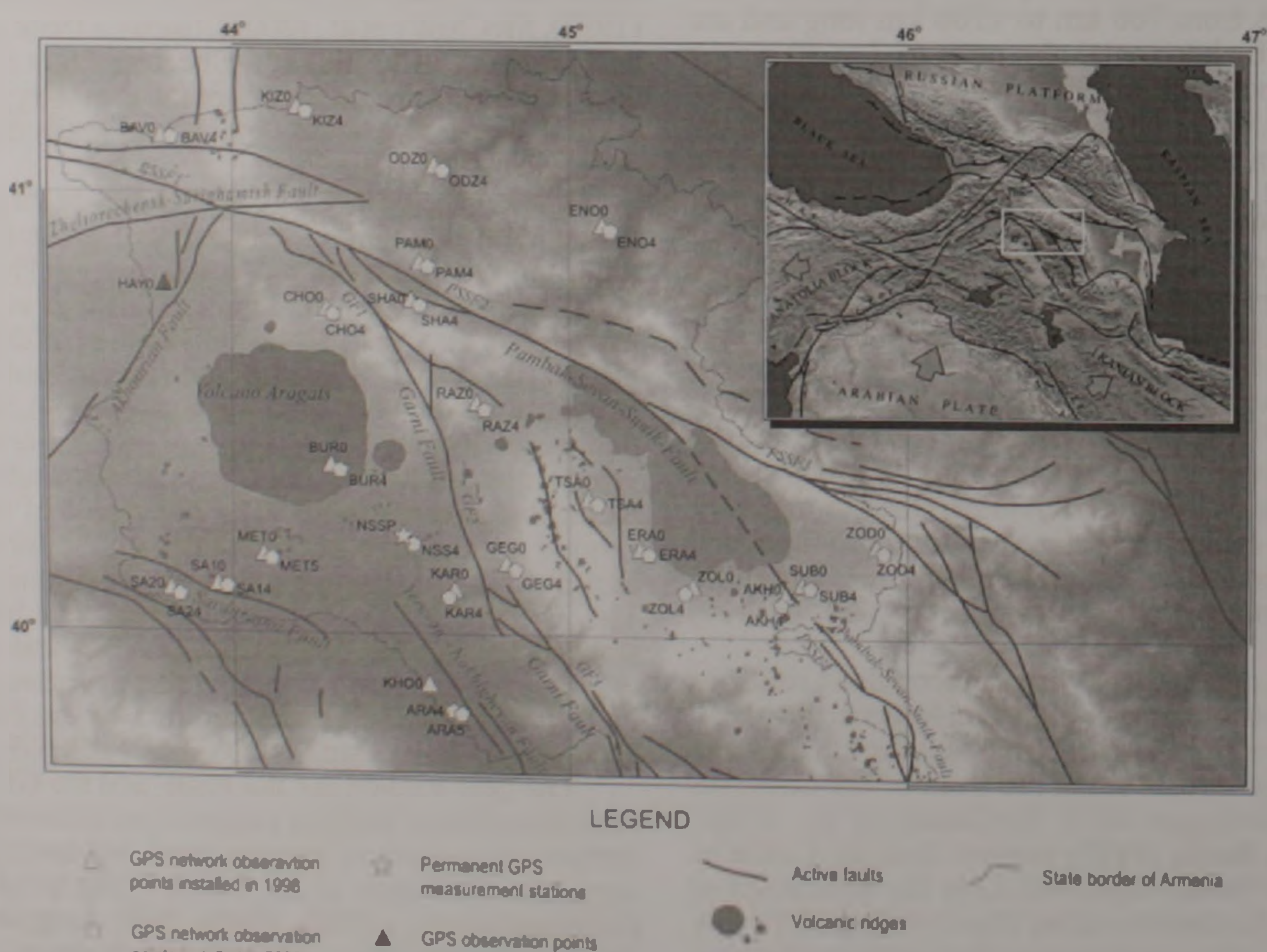


Fig.1. Locations of GPS network points.

2. The area located between GF and PSSF (Fig.1). Linear zones of intense areal Holocene-Quaternary volcanism and the volcano-tectonic depression of Lake Sevan occupy the inner part of this area. The extensive development of collision volcanism in Armenia, within the areas of predominant and intense shortening, poses a fascinating geodynamic problem, and GPS evidence may be important to resolve it. The National Park of Lake Sevan is located in the limits of this zone. In the historical time, the segments of GF and PSSF, bordering the area, generated $M=7.0-7.5$ earthquakes accompanied by volcanic eruptions (Karakhanyan et al, 2004).

3. The triangular area outlined by the AF and GF faults (Fig.1). Aragats, a large stratovolcano, is situated in the central part of this area. According to the geodynamic models (Karakhanyan et al, 1997), the Arabian plate moves the triangular Aragats block to the north. The GF, Sardarapat fault (SF) and Yerevan fault (YF) are located in the southern part of the area (Fig. 1). These faults are proximal to the vital infrastructure facilities in Armenia. The Sardarapat Fault is 13 km far from the Armenian Nuclear Power Plant. The Yerevan Fault (YF) represents a zone that is not clearly identified on the surface; this fault stretches through the southern part of the Yerevan City (population of 1.5 million). The fault has displayed seismic activity as $M=3.0-4.6$ earthquakes recurring in 10-15 years intervals. Estimates of recent deformation rates in the listed fault zones can be essential for seismic hazard and risk assessment for the territory of Armenia.

In 2003, new points were installed and measured

within a few meters distance from the observation points installed in 1998. The need for re-installation was determined by total destruction or partial damage of the 1998 points by local population. Point HAY0 was destroyed completely, while points AKH0, ERA0, ZOL0 and SUB0 were found damaged but still recoverable. To ensure secure operation of our network, we installed duplicates for all points in 2003.

In the duplicating net, new points were installed 10-15m far from the old ones. The installation technique provided for masking the points as much as feasible. The benchmarks we used are shown in Fig.2. They were located under the ground surface and masked with a concrete layer during the period between the measurements. Another difference of the new reference stations is that the GPS receiver antenna is not placed on a tripod, as earlier done, but rigidly fastened on the benchmark with a special rod. The trial tests performed by the French colleagues show that GPS satellite signals reflected by the surface almost do not influence the credibility of the obtained result. Therefore, application of the new type benchmarks (Fig.2) can help to avoid common uncertainties generated during GPS measurements by means of a tripod (tripod installation, tripod vibration, etc.).

To reference the old points to the new ones, concurrent GPS measurements were performed for both during the 2003 session.

Details on the measurements and data processing

The GPS measurement sessions were conducted in 1998, 2000 and 2003. Graphs 1,2 and 3 demonstrate the measurement values. The measurements were made by means of dual-frequency phase GPS receivers *Ashtech Z12* and *Ashtech ZX* equipped with *Chock Ring* type *Ashtech* antennas.

Definition of network point coordinates and of the rates of their motion was accomplished by use of software packages *GAMIT 10.05* (King and Bock, 2001)

Table 1

The timetable of measurements in the GPS network in 1998

| Site | GPS observation days in the year of 1998 | | | | | | | |
|------|------------------------------------------|-----|-----|-----|-----|-----|-----|-----|
| | 262 | 263 | 265 | 266 | 268 | 269 | 271 | 272 |
| KAR0 | x | x | | | | | | |
| KHO0 | x | x | | | | | | |
| METO | x | x | | | | | | |
| SA10 | x | x | | | | | | |
| SA20 | x | x | | | | | | |
| AKH0 | | | x | x | | | | |
| ZOL0 | | | x | x | | | | |
| ERA0 | | | x | x | | | | |
| SUB0 | | | x | x | | | | |
| ZOD0 | | | x | x | | | | |
| ENO0 | | | x | x | x | x | | |
| BUR0 | x | x | x | x | x | x | x | |
| ODZ0 | | | | | x | x | x | |
| GEG0 | | | | | x | x | | |
| PAM0 | | | | | x | x | | |
| RAZ0 | | | | | x | x | | |
| TSA0 | | | | | x | x | | |
| BAV0 | | | | | | x | | x |
| CHO0 | | | | | | x | | x |
| HAY0 | | | | | | x | | x |
| KIZ0 | | | | | | x | | x |
| SHAO | | | | | | x | | x |

Fig.2: Benchmarks of the duplicating GPS network points

Table 2

The timetable of measurements in the GPS network in 2000

| Site | GPS observation days in the year of 2000 | | | | | | | | | | | | | | | | | | | | | |
|------|------------------------------------------|-----|-----|-----|-----|-----|-----|-----|-----|-----|-----|-----|-----|-----|-----|-----|-----|-----|-----|-----|-----|-----|
| | 186 | 187 | 189 | 190 | 192 | 193 | 195 | 196 | 200 | 201 | 203 | 204 | 206 | 207 | 209 | 210 | 214 | 215 | 217 | 218 | 220 | 221 |
| SA10 | X | X | | | | | | | | | | | | | | | | | | | | |
| SA20 | X | - | X | | | | | | | | | | | | | | | | | | | |
| KH00 | | | X | X | | | | | | | | | | | | | | | | | | |
| METO | | | X | X | | | | | | | | | | | | | | | | | | |
| BUR0 | | | | | X | X | | | | | | | | | | | | | | | | |
| GEG0 | | | | | X | - | | | | | | | | | | | | | | | | |
| KAR0 | | | | | | | X | X | | | | | | | | | | | | | | |
| RAZ0 | | | | | | | X | X | | | | | | | | | | | | | | |
| BAV0 | | | | | | | | | X | X | | | | | | | | | | | | |
| KIZ0 | | | | | | | | | X | X | | | | | | | | | | | | |
| ODZ0 | | | | | | | | | | | X | X | | | | | | | | | | |
| PAM0 | | | | | | | | | | | X | X | | | | | | | | | | |
| CHO0 | | | | | | | | | | | | X | X | | | | | | | | | |
| SHAO | | | | | | | | | | | | X | X | | | | | | | | | |
| ENO0 | | | | | | | | | | | | | X | X | | | | | | | | |
| ERA0 | | | | | | | | | | | | | X | X | | | | | | | | |
| TSA0 | | | | | | | | | | | | | | X | X | | | | | | | |
| ZOD0 | | | | | | | | | | | | | | | X | X | | | | | | |
| ZOLO | | | | | | | | | | | | | | | | X | X | | | | | |
| SUB0 | | | | | | | | | | | | | | | | | X | X | | | | |
| AKHO | | | | | | | | | | | | | | | | | | | X | X | | |

Table 3

The timetable of measurements in the GPS network in 2003

| Site | GPS observation days of the year of 2003 | | | | | | | | | | | | | |
|------|------------------------------------------|-----|-----|-----|-----|-----|-----|-----|-----|-----|-----|-----|-----|-----|
| | 177 | 178 | 180 | 181 | 183 | 184 | 186 | 187 | 189 | 190 | 192 | 193 | 195 | 196 |
| BAV0 | X | X | | | | | | | | | | | | |
| BAV4 | - | - | | | | | | | | | | | | |
| ODZ0 | X | X | | | | | | | | | | | | |
| ODZ4 | X | X | | | | | | | | | | | | |
| ZOD0 | X | X | | | | | | | | | | | | |
| ZOD4 | X | X | | | | | | | | | | | | |
| KIZ0 | | | X | X | | | | | | | | | | |
| KIZ4 | | | X | X | | | | | | | | | | |
| PAM0 | | | - | X | | | | | | | | | | |
| PAM4 | | | X | X | | | | | | | | | | |
| SURO | | | X | X | | | | | | | | | | |
| SUB4 | | | X | X | | | | | | | | | | |
| AKHO | | | | | X | X | | | | | | | | |
| AKH4 | | | | | X | X | | | | | | | | |
| CHO0 | | | | | X | X | | | | | | | | |
| CHO4 | | | | | X | X | | | | | | | | |
| SHA0 | | | | | X | X | | | | | | | | |
| SHA4 | | | | | X | X | | | | | | | | |
| NSS4 | X | X | X | X | X | X | | | X | X | X | X | X | X |
| ARA4 | | | | | | | X | X | X | X | X | X | X | X |
| ARAS | | | | | | | X | X | X | X | X | X | X | X |
| ENO0 | | | | | | | X | X | X | X | X | X | X | X |
| ENO4 | | | | | | | X | X | X | X | X | X | X | X |
| ZOLO | | | | | | | X | X | | | | | | |
| ZOL4 | | | | | | | X | X | | | | | | |
| ERA0 | | | | | | | | | X | X | | | | |
| FRA4 | | | | | | | | | X | X | | | | |
| GEG0 | | | | | | | | | X | X | | | | |
| GEG4 | | | | | | | | | X | X | | | | |
| SA20 | | | | | | | | | X | X | | | | |
| SA24 | | | | | | | | | X | X | | | | |
| KAR0 | | | | | | | | | | | X | X | | |
| KAR4 | | | | | | | | | | | X | X | | |
| SA10 | | | | | | | | | | | X | X | | |
| SA14 | | | | | | | | | | | X | X | | |
| TSA0 | | | | | | | | | | | X | X | | |
| TSA4 | | | | | | | | | | | X | X | | |
| BUR0 | | | | | | | | | | | | | X | X |
| BUR4 | | | | | | | | | | | | | X | X |
| METO | | | | | | | | | | | | | X | X |
| MET4 | | | | | | | | | | | | | X | X |
| RAZ0 | | | | | | | | | | | | | X | X |
| RAZ4 | | | | | | | | | | | | | X | X |

and GLOBK 10.0 (Herring, 2001). The analysis involved permanent stations BAHR and KIT3 in the International GPS Service for Geodynamics (IGS), BOR1, GLSV,

Table 4

Velocities of motions of the GPS network points in ITRF 2000: Site – names of stations; Long E, Lat N – Cartesian coordinates; E-Vel, N-Vel – the eastern and northern components of motion velocity vectors of the points, respectively (mm/yr); σ_E , σ_N – uncertainties (mm/yr); ρ_{EN} – Correlation coefficient between the east and north uncertainties

| Site | Long E | Lat N | E-Vel | σ_E | N-Vel | σ_N | ρ_{EN} |
|------|--------|--------|-------|------------|-------|------------|-------------|
| AKHO | 45.645 | 40.099 | 2.39 | 0.84 | 8.03 | 0.54 | 0.005 |
| BAVO | 43.782 | 41.121 | 1.14 | 0.58 | 5.82 | 0.59 | -0.035 |
| BUR0 | 44.287 | 40.381 | 0.89 | 0.56 | 6.1 | 0.41 | -0.054 |
| CHO0 | 44.276 | 40.736 | 0.95 | 0.62 | 9.2 | 0.47 | -0.023 |
| ENO0 | 45.094 | 40.92 | 2.45 | 0.81 | 7.06 | 0.65 | -0.04 |
| ERA0 | 45.209 | 40.198 | 3.04 | 0.54 | 7.57 | 0.42 | -0.033 |
| GEG0 | 44.81 | 40.16 | 3 | 0.5 | 6.85 | 0.38 | -0.039 |
| KAR0 | 44.657 | 40.101 | 1.57 | 0.79 | 6.71 | 0.71 | -0.019 |
| KHO0 | 44.575 | 39.881 | 4.05 | 1.18 | 9.79 | 1.04 | -0.016 |
| KIZ0 | 44.19 | 41.185 | 1.29 | 0.42 | 4.52 | 0.38 | -0.019 |
| METO | 44.091 | 40.178 | 0.89 | 0.82 | 6.91 | 0.72 | -0.034 |
| NSSP | 44.503 | 40.226 | 2.17 | 0.41 | 0.32 | 0.21 | -0.01 |
| ODZ0 | 44.593 | 41.055 | 2.46 | 0.41 | 7.14 | 0.32 | -0.016 |
| PAM0 | 44.55 | 40.84 | 1.62 | 0.43 | 7.42 | 0.34 | -0.02 |
| RAZ0 | 44.718 | 40.52 | 1.97 | 1.25 | 5.1 | 1.25 | -0.021 |
| SA10 | 43.951 | 40.108 | 1.69 | 0.52 | 9.04 | 0.36 | -0.035 |
| SA20 | 43.807 | 40.097 | 1.28 | 0.9 | 6.22 | 0.84 | -0.022 |
| SHAO | 44.528 | 40.753 | 2.04 | 0.61 | 6.48 | 0.45 | -0.025 |
| SUB0 | 45.686 | 40.117 | 3.47 | 0.59 | 8.67 | 0.48 | -0.017 |
| TSA0 | 45.055 | 40.307 | 3.16 | 0.67 | 8.18 | 0.59 | -0.025 |
| ZODO | 45.908 | 40.204 | 5.1 | 0.92 | 8.53 | 0.91 | -0.01 |
| ZOLO | 45.367 | 40.114 | 3.16 | 0.66 | 8.55 | 0.5 | -0.016 |

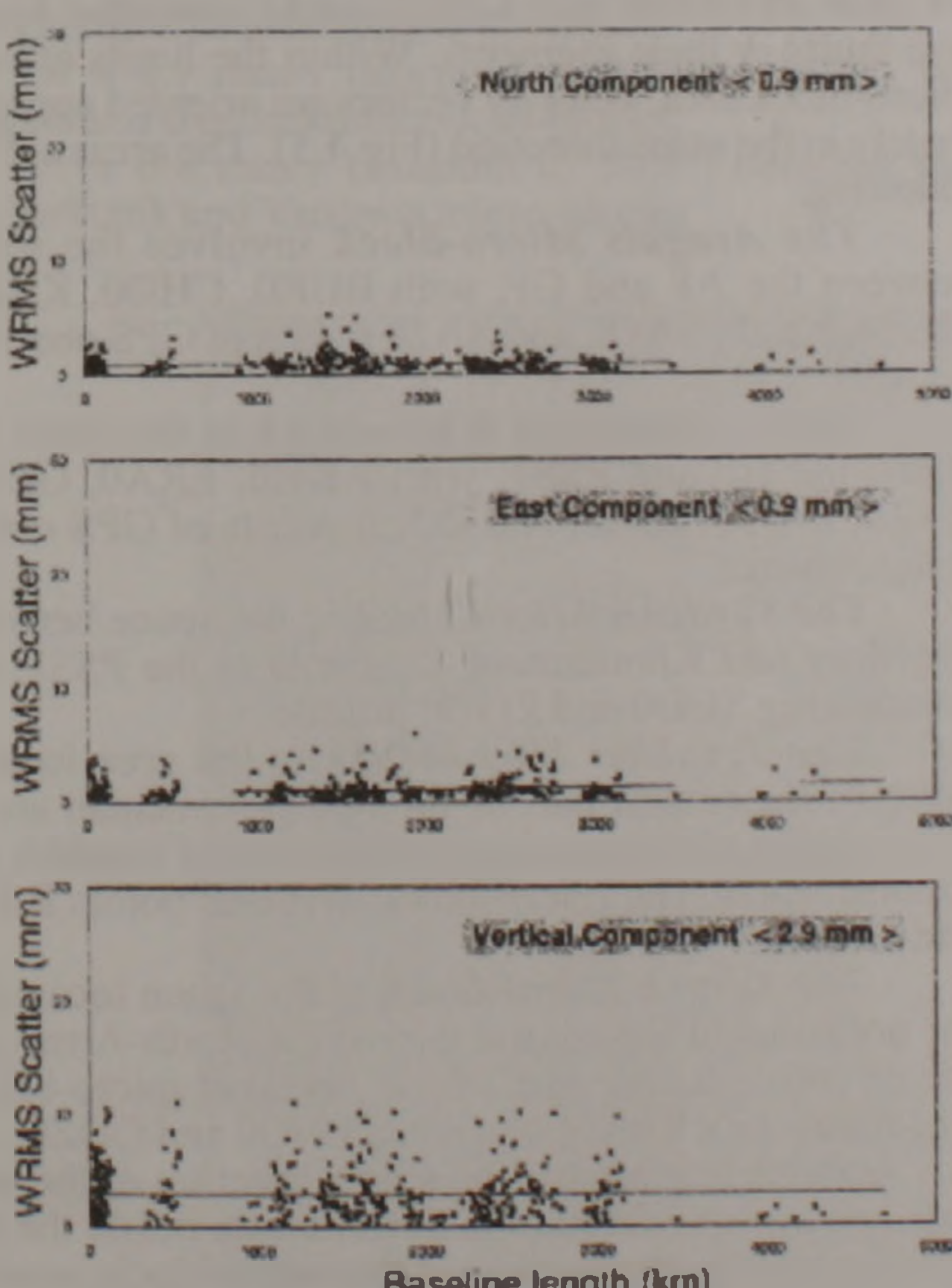


Fig.3: Baseline component repeatabilities versus baseline length. The first, second and third rows are for the north, east and vertical components.

MATE, NICO, WTZR, ZECK and ZIMM in the European Reference Frame network (EUREF), NSSP from the Mediterranean GPS Network (MGN), NSSS from the Survey of Israel / Tel Aviv University / Royal Jordanian Geographic Centre (SOI-TAU-RJGC), and RAMO from the Southern California Integrated GPS Network (SCIGN). The calculation of positions and motion rates of the points was made in the ITRF2000 system. Table 4 lists the names, geographic coordinates and motion rates for the points of our GPS network in ITRF2000.

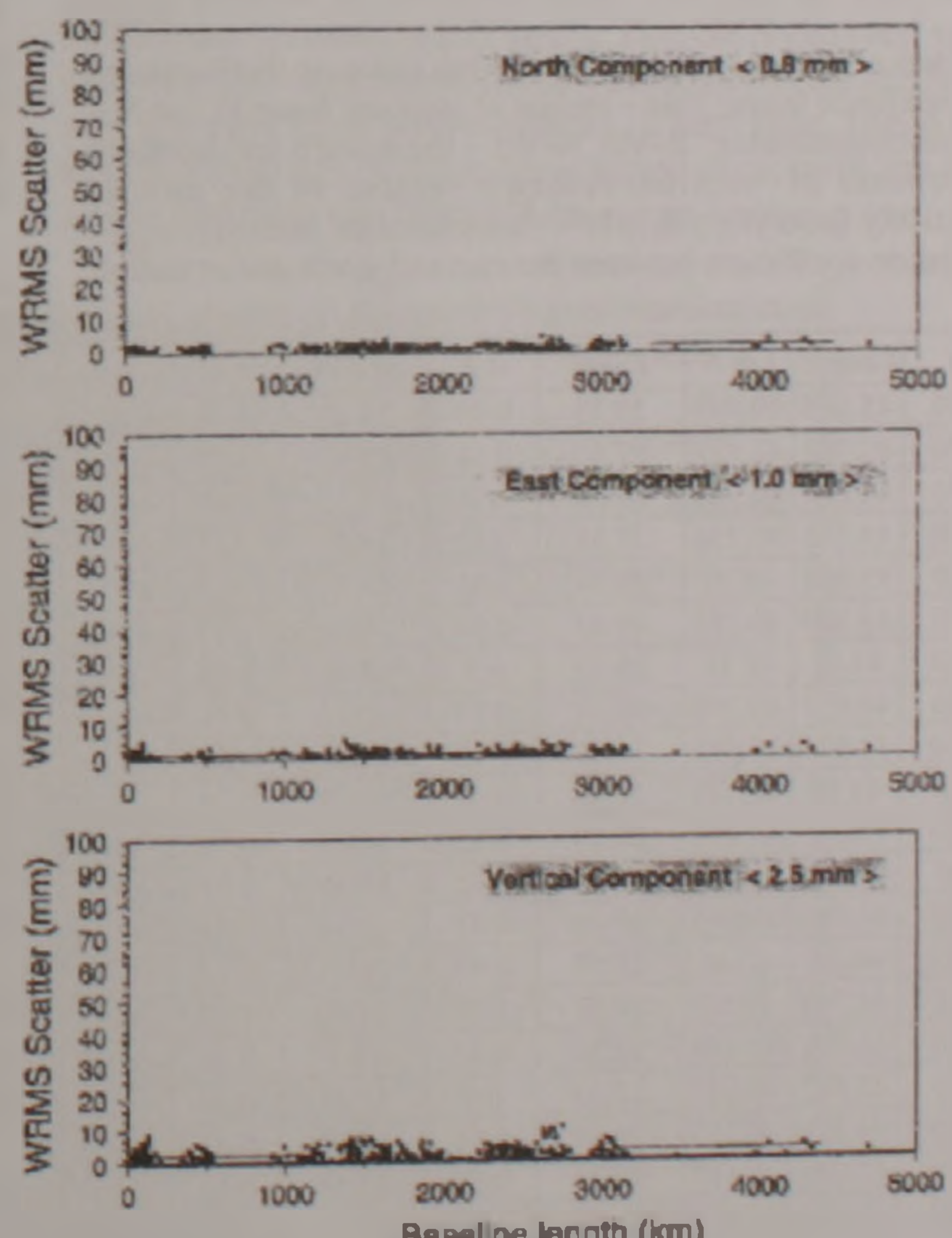
Table 3 shows that measurements of the GPS network in 2003 were conducted concurrently for the new and old points. This improved the accuracy of measurements. The representativeness of the derived coordinates in case of orbit relaxed biases fixed is shown in Fig.3.

GPS velocity field in the Eurasia-fixed reference frame

To study deformation rates and directions, we fixed the frame at the Eurasian plate, i.e., this plate was assumed not moving. The fixation at the Eurasian plate was achieved by subtracting from the vector values the velocities of points derived in ITRF2000, Absolute Rotation Pole of Eurasia (Altamimi et al., 2002). Fig.4 demonstrates velocity vectors for the offsets of the GPS network points relative to Eurasia, and Table 5 lists their names, geographic coordinates and motion rates.

The obtained deformation rates can be interpreted based on the two assumptions:

1. The territory of Armenia is split into a few rigid non-deformed micro-blocks that move one relative to the other under the impact of the northern drift of the Arabian plate (Balassanian et al., 1999 a,b,c). If this is the case, the micro-blocks must display individual mo-



tion velocities and azimuths, while the entire deformation measured by GPS receivers must be realized at micro-block boundaries.

2. The northern drift of the Arabian plate produces

motions along active faults in Armenia, while areas confined by these faults undergo elastic deformation, the rate and the character of which can change in space and time.

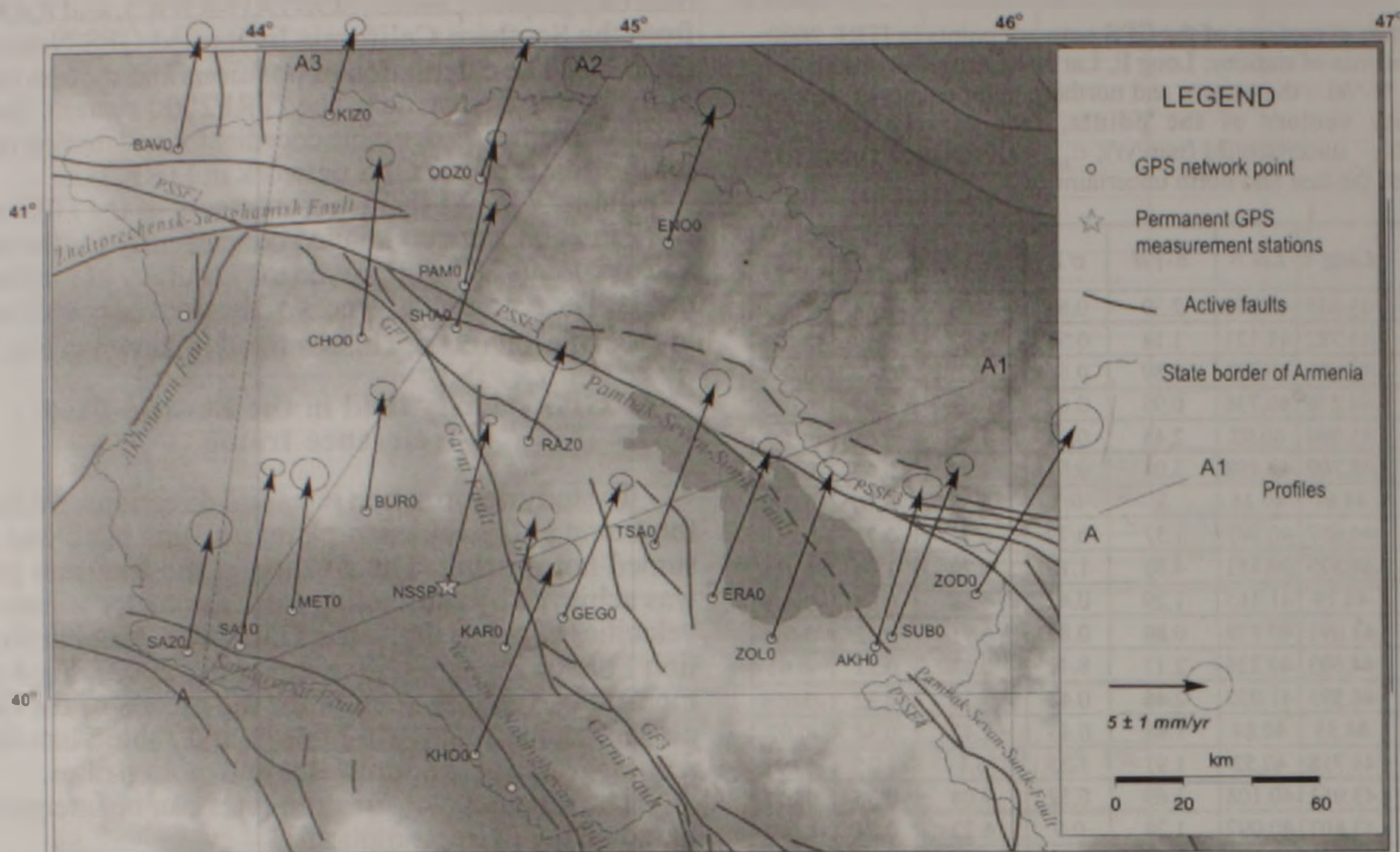


Fig.4. GPS horizontal velocities and their confidence ellipse in a Eurasia-fixed reference frame

Below we will try to consider the applicability of the obtained GPS data using both of the models

Table 5

Velocities of motions of the GPS network points in the Eurasian-fixed reference frame. Site – names of stations; Long E, Lat N – Cartesian coordinates; E-Vel, N-Vel – the eastern and northern components of motion velocity vectors of the points, respectively (mm/yr); yE, yN – uncertainties (mm/yr); c_{EN} – Correlation coefficient between the east and north uncertainties

| Site | Long E | Lat N | E-Vel | σ_E | N-Vel | σ_N | c_{EN} |
|------|--------|--------|-------|------------|-------|------------|----------|
| AKHO | 45 645 | 40 099 | 29.23 | 0.84 | 16.82 | 0.54 | 0.005 |
| BAV0 | 43 782 | 41 121 | 27.67 | 0.58 | 15.02 | 0.59 | -0.035 |
| BUR0 | 44 287 | 40 381 | 27.56 | 0.56 | 15.19 | 0.41 | -0.054 |
| CHO0 | 44 276 | 40 736 | 27.58 | 0.62 | 18.29 | 0.47 | -0.023 |
| EN00 | 45 094 | 40 92 | 29.14 | 0.81 | 15.97 | 0.65 | -0.04 |
| ERA0 | 45 209 | 40 198 | 29.83 | 0.54 | 16.46 | 0.42 | -0.033 |
| GEG0 | 44.81 | 40.16 | 29.75 | 0.5 | 15.82 | 0.38 | -0.039 |
| KAR0 | 44 657 | 40 101 | 28.31 | 0.79 | 15.72 | 0.71 | -0.019 |
| KHO0 | 44 575 | 39 881 | 30.81 | 1.18 | 18.81 | 1.04 | -0.016 |
| KIZ0 | 44 19 | 41 185 | 27.86 | 0.42 | 13.63 | 0.38 | -0.019 |
| MET0 | 44 091 | 40 178 | 27.56 | 0.82 | 16.04 | 0.72 | -0.034 |
| NSSP | 44 503 | 40 226 | 28.88 | 0.32 | 17.45 | 0.21 | -0.01 |
| ODZ0 | 44 593 | 41 055 | 29.09 | 0.41 | 16.16 | 0.32 | -0.016 |
| PAM0 | 44.55 | 40.84 | 28.27 | 0.43 | 16.45 | 0.34 | -0.02 |
| RAZ0 | 44 718 | 40 52 | 28.67 | 1.25 | 14.09 | 1.25 | -0.021 |
| SA10 | 43 951 | 40 108 | 28.36 | 0.52 | 18.2 | 0.36 | -0.035 |
| SA20 | 43 807 | 40 097 | 27.93 | 0.9 | 15.41 | 0.84 | -0.022 |
| SHAO | 44.528 | 40.753 | 28.69 | 0.61 | 15.52 | 0.45 | -0.025 |
| SUB0 | 45 686 | 40 117 | 30.31 | 0.59 | 17.45 | 0.48 | -0.017 |
| TSA0 | 45 055 | 40 307 | 29.92 | 0.67 | 17.1 | 0.59 | -0.025 |
| ZODO | 45 908 | 40 204 | 31.95 | 0.92 | 17.26 | 0.91 | -0.01 |
| ZOLO | 45 367 | 40 114 | 29.97 | 0.66 | 17.4 | 0.5 | -0.016 |

The model of rigid micro-blocks

Analyzing the obtained data from this standpoint, we have identified micro-block-areas separated by active faults or their segments. Within the limits of each micro-block area, velocity vectors are oriented approximately in the same direction (Fig.4,5). The areas are the following:

• **The Aragats Micro-block** involves the space between the AF and GF, with BUR0, CHO0, KAR0, MET0, NSSP, SA10, and SA20 points of GPS observations;

• **The Gegharkunik Micro-block** is the space between the GF and PSSF, with AKH0, ERA0, GEG0, RAZ0, SHA0, TSA0, and ZOL0 points of GPS observations inside;

• **The Vardenis Micro-block** is the space between the Mrav and Khonarassar segments of the PSSF, encompassing SUB0 and ZOD0 points;

• **The Javakhet Micro-block** is the area located north of the central part of the North-Armenian arc of active faults corresponding to the zone of Javakhk extension faults. The micro-block involves points BAV0 and KIZ0;

• **The Tavush Micro-block** is the space located to the northeast of the central part of the North-Armenian arc of active faults, east of the Javakhet micro-block. The micro-block involves points EN00 and ODZ0.

Considering almost the same direction of the vectors, we assume absence of deformation inside the micro-blocks, i.e., the rigidity of the micro-block massifs. This allows us to apply averaging to derive a velocity vector for each identified micro-block relative to Eurasia

and consider the model of rigid micro-block deformation for the studied area.

Table 6 presents average motion velocities and velocity azimuths for each of the micro-blocks relative to Eurasia, and Fig 5 shows the averaged velocity vectors.

The north-northeastern drift of the Aragats micro-block with an azimuth of 10.2° can generate the north-northeastern motion of the Gegharkunik micro-block and the Vardenis micro-block at the azimuths of 20.3° and 26.5° , respectively (Fig.5). Concurrent motion of the

Average velocities of motions for inelastic blocks in the Eurasian-fixed reference frame: V_{Eaver} , V_{Naver} – eastern and northern components of the average block motion velocity, respectively; y_{Eaver} , y_{Naver} – averaged uncertainties; Speed – average velocity of blocks; Angle – azimuth

| Micro-block Name (Stations in block) | V_E _{aver.} (mm/year) | V_N _{aver.} (mm/year) | σE _{aver.} (mm/year) | σN _{aver.} (mm/year) | Speed | Angle (degree) |
|---------------------------------------------------------------------|-------------------------------------|-------------------------------------|------------------------------------------|------------------------------------------|-------|-------------------|
| Aragats (BUR0, CHO0, KAR0, MET0, NSSP, SA10, SA20) | 1.35 | 7.51 | 0.65 | 0.53 | 7.63 | 10.2 |
| Gegharkunik (AKH0, ERA0, GEG0, RAZ0, SHA0, TSA0, ZOL0) | 2.68 | 7.25 | 0.72 | 0.59 | 7.73 | 20.3 |
| Vardenis (SUB0, ZOD0) | 4.29 | 8.60 | 0.76 | 0.70 | 9.61 | 26.5 |
| Javakhet (BAV0, KIZ0) | 1.22 | 5.17 | 0.50 | 0.49 | 5.31 | 13.2 |
| Tavush (ENO0, ODZ0) | 2.46 | 7.10 | 0.61 | 0.49 | 7.51 | 19.1 |

Aragats, Gegharkunik and Vardenis micro-blocks can in turn cause the Javakhet and Tavoush micro-blocks to move north-northeasterly with the azimuths of 13.2° and 19.1° , respectively (Fig.5). Compressive deformation recorded for the area between the Aragats and Javakhet micro-blocks has an azimuth of 3.3° and a rate of 2.3 ± 0.6 mm/y. In the meantime, deformation recorded between the remaining micro-blocks is extensional (Fig.5) and corresponds to:

2.1 ± 0.6 mm/y (azimuth of 32.7°) between the Javakhet and Tavoush micro-blocks,

1.4 ± 0.7 mm/y (azimuth of 78.9°) between the Aragats and Gegharkunik micro-blocks,

2.1 ± 0.8 mm/y (azimuth of 50.0°) between the Gegharkunik and Vardenis micro-blocks

3.1 ± 0.8 mm/y (azimuth of 69.7°) between the Aragats and Vardenis micro-blocks.

Interpreting the listed velocities from the standpoint of the rigid micro-block model, we can suggest the following:

- The North-Armenian tectonic arc represents a boundary, to both sides of which deformation rates change significantly (Fig.5).

- The boundary between the Aragats and Javakhet micro-blocks is located near the tip of the North-Armenian tectonic arc (Fig.5). The GPS-derived velocities record compressive deformation between the Aragats and the Javakhet micro-blocks. Therefore, the Aragats micro-block can be a wedge-shaped area, with the wedge angle forming the North-Armenian tectonic arc.



Fig.5: Distribution of rigid, non-deformable micro-blocks of lithosphere in central and northern Armenia. Average horizontal GPS velocities of block motions

While moving, the Aragats micro-block pushes the Gheharkounik and the Vardenis micro-blocks towards the northeast. This suggestion is supported by increasingly higher motion azimuths recorded eastwardly for the Gheharkounik and Vardenis micro-blocks in comparison to the azimuth of motion of the Aragats micro-block (Fig.5).

About 30% of the Aragats micro-block motion velocity is consumed in the area of the tip of the North-Armenian tectonic arc.

In this model, we assumed non-deformability of the micro-blocks and realization of the deformation entirely on micro-block boundaries along active faults. In many aspects, the model is similar to, and to a certain extent repeats the geodynamic model suggested by Karakhanyan et al (1997). It demonstrates generalized characteristics of the lithosphere deformation field in the north of Armenia relative to the Eurasian continental plate. However, the proposed model appears in serious conflict with the tectonic, seismic and geodynamic evidence, obtained by the latest field studies (Philip et al, 2001; Avagyan, 2001; Karakhanyan et al, 2004). Principally, this conflict is related to the assumed complete release of deformation on micro-block boundaries, i.e., in active fault zones only. Large areas of Quaternary and Holocene volcanism within the Aragats, Javakhet, Gheham, and Vardenis micro-blocks attest to active extension in this region (Fig.1). Smaller active faults, also present within each of the micro-blocks, display both tectonic, and seismic activity by frequent weak and middle-size earthquakes in the magnitude range of $M=1.5-4.5$. These structures all have resulted from intense deformations inside the micro-blocks.

There is another problem related to the identification of rigid micro-blocks. Most of the micro-blocks can not be fully outlined by credibly identifiable faults (Fig. 1). Our attempts to use a different geometry of the micro-blocks faced an incompatibility with the pattern of distribution of motion directions derived by the GPS data. Continued hierachic reduction of the dimensions of the rigid micro-blocks is not supported geologically and contradicts the GPS data. To study the character of intra-micro-block deformations, we will consider the next model below.

The models of distributed deformation

The analysis of general distribution of velocity vectors in the region indicates continuous decrease of deformation rates from the south to the north (Reilinger, Barka, 1997; McClusky et al., 2000). A considerable share of the deformation created by the drifting Arabian plate is absorbed by the system of right-lateral strike-slip faults in Eastern Turkey and Northern Iran, including the Chaldiran, Karayaz, and Siesh-Cheslimch Khoy-North Tabriz faults (Reilinger, Barka, 1997; McClusky et al., 2000, Barka and Kadinsky-Cade, 1988; Berberian, 1997, Karakhanyan et al., 2004).

Our analysis of GPS network data in Armenia shows that in the west-to-east direction deformation field azimuths change regularly from N-NE to E-NE (Fig. 4). This can be interpreted as extension conditions originating at the site bounded by the GF and the PSSF faults.

When projected on Line A-A1 (Fig.4), displacement velocity vectors allow us to suggest that extension increases in the northeastern direction (Fig.6a). Projec-

tion of the velocity vectors on Lines A-A2 and A-A3 (Fig. 4, 6b, 6c) reveals sizeable extension in the Sardarapat Fault Zone. Deformation in the central part of the Aragats site bounded by the GF, AF and SF faults, is characterized by alternating increases and decreases of motion velocities for stations SA10, MET0, NSSP, BUR0 and CHO0 (Fig.6a, 6c), attesting to the interchange between compression and extension deformations in the region. In the tip part of the North-Armenian tectonic arc, deformation in the area of crossing between two right-lateral, and two left-lateral strike-slip faults is defined by velocity vectors of stations CHO0, BAV0 and KIZ0 and characterized as compressive deformation (Fig.6a).

Therefore, the model of distributed velocities indicates that deformations are present also inside the areas bounded by the faults, and the micro-blocks we identified are not homogeneous. We conclude that the concept of micro-block rigidity is questionable itself; hence, application of the model of rigid micro-blocks must be limited to an averaged regional characterization of large region geodynamics.

Deformation rates in the fault zones

To estimate deformation rates in active fault zones, the proximal stations (located as close to the faults as the available GPS network permitted) were used only. The technique applied for this purpose was to measure velocity vectors for stations on one side of a fault with reference to a fixed station on the opposite side. In such case, the analysis was based on station motion velocities defined in the ITRF2000 system (Table 4).

Figure 7 shows velocity vectors in the GPS network relative to station CHO0. The distribution of slip velocity vectors within the site outlined by the Garni Fault and the Pambak-Sevan-Syunik Fault is peculiar (Fig.7). The velocity vectors of the stations located at the margin of this site, near to the Garni Fault (SHA0, RAZ0, GEG0) and Pambak-Sevan-Syunik Fault (AKH0), are oriented in parallel to these faults (Fig.7). Moreover, the directions of these vectors are well consistent with the geological estimates of deformation inside the mentioned fault zones. This allows us to suggest that the considered points fall within the Garni and Pambak-Sevan-Syunik fault zones and are subject to their respective deformation regimes. In the meantime, slip velocity vectors of the points situated in the central part of the site (TSA0, ERA0, and ZOL0) are of more latitudinal orientation as compared to the ones derived for the marginal stations (Fig.7). This effect can be explained by latitudinal extension in the centre of the site, which is also supported by the geological evidence.

The data from stations CHO0, SHA0, NSSP, RAZ0, KAR0, and GEG0 suggest that different segments of the GF have diverse kinematics. As calculated by the GPS data, the kinematics of the GF1 segment must correspond to right-lateral strike-slip at a rate of 3.0 ± 0.6 nm/y (Fig.8).

The GF2 segment of the Garni Fault, the existence of which is much argued, is of particular interest. Much of the argument can be due to poor identification of this segment on the surface as the land is under intense agricultural cultivation and young lava flows cover the fault zone. In this work we use a tectonic model that accounts for this segment (Fig.1). However, there are alternative tectonic models that do not include the GF2 segment, or

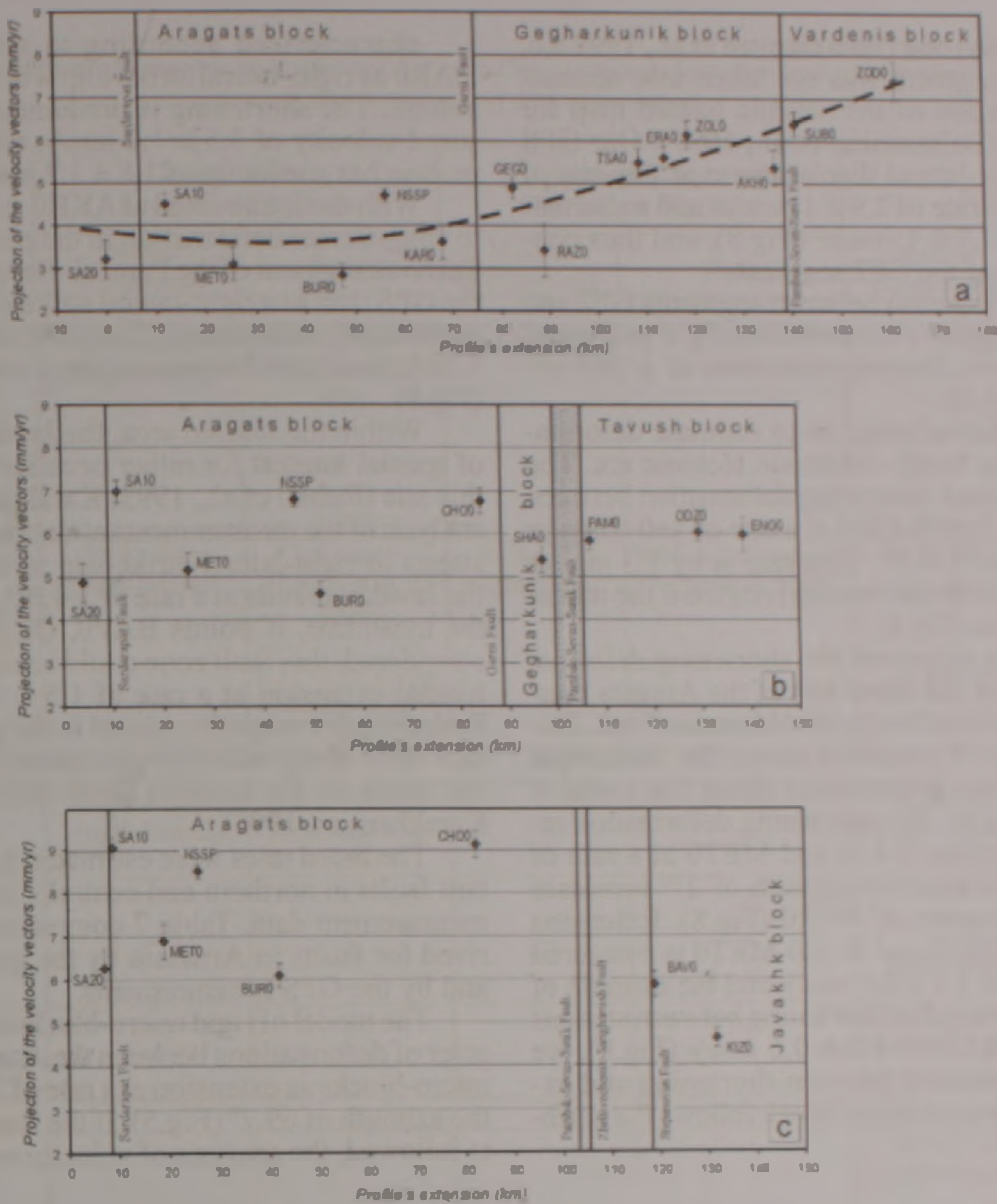


Fig.6: Distribution of velocities for the motions of the GPS network points projected onto profiles: a – Profile A-A1, b – Profile A-A2; c – Profile A-A3.



Fig.7. GPS horizontal velocities and their confidence ellipses in a CHO0-fixed reference frame.

mark it as a supposed one (Balassanyan et al., 1999 a,b, and c). The GF2 segment was not taken into account during the preparation of the seismic hazard map for Armenia in 1994 (Balassanian et al., 1997). Our GPS studies record right-lateral displacement at this site of the Garni Fault at a rate of 2.9 ± 1 mm/yr and a shortening component of 1.7 ± 1 mm/yr (Fig.8), and thus confirm the existence of the GF2 segment.

In the zone of junction between segments GF2 and GF3, where geological evidence identify a pull-apart basin structure, we observe extension at a rate of 1.4 ± 0.8 mm/yr (Fig.8).

Our GPS studies allowed us to estimate deformation in the tip of the North-Armenian tectonic arc. The calculations determined shortening deformation between stations CHO0 and BAV0-KIZ0 at a rate of 4 ± 0.6 mm/yr (Fig.8) and azimuth of -4.5° . This rate is by 1.3 mm/yr greater compared to the one we derived from the model of rigid micro-blocks (Fig.5).

The alternating extension and shortening deformations are recorded in the inner part of the Aragats massif bordered by the Garni Fault and Akhourian Fault. Stations SA20 and SA10 straddled across the Sardarapat Fault record extensive deformation along it at a rate of 2.7 ± 0.9 mm/yr (Fig.8). The shortening deformation recorded between stations SA10 and MET0 at a rate of 2.7 ± 0.9 mm/yr and with the azimuth of 27° increases farther towards the point of BUR0 (Fig.8). Extension between stations CHO0 and BUR0-MET0 is measured to have a velocity of 3.1 ± 0.6 mm/yr and the azimuth of -1° (Fig.8). Considering that shortening between stations CHO0 and BAV0-KIZ0 is 4.0 ± 0.6 mm/yr (Fig.8), we derive that the alternation between shortening and extension inside the Aragats micro-block follows the north-to-south direction

characterized according to stations KHO0 and KAR0 as right-lateral strike-slip with a shortening component. The shortening is predominant, with the measured velocity of 3.5 ± 1.2 mm/yr, while the strike-slip motion has a velocity of 1.8 ± 1.2 mm/yr (Fig.8).

With the frame fixed at AKH0 station, it is possible to characterize deformation in the zone of the Artanish-Tskhouk segment of the Pambak-Sevan-Syunik Fault by the GPS data as a right-lateral strike-slip motion with an extensional component. The strike-slip motion rate is 1.2 ± 0.9 mm/yr, and extension has a rate of 2.5 ± 0.9 mm/yr (Fig.8).

Within the studied area, the Javakhet Fault Zone is of special interest for rather peculiar seismic regime at this site (Rebaï. et al., 1993; Karakhanyan, 1995). Our analysis of the measurements at stations BAV0 and KIZ0 attests to right-lateral strike-slip motion in the area of the Javakhet faults at a rate of 1.4 ± 0.6 mm/yr (Fig.8). In the meantime, if points BAV0, ODZ0 and ENO0 are considered, this fault zone could be also assigned a latitudinal extension at a rate of 1.5 ± 0.8 mm/yr (Fig.8). Probably, this might be related to the presence of extension faults along with the right-lateral strike-slip faults in the limits of the Javakhet Zone (Rebaï. et al., 1993; Karakhanyan, 1995).

The listed rates were estimated for the most important faults in northern and central Armenia by the GPS measurement data. Table 7 compares the slip rates derived for faults in Armenia by the geological methods and by the GPS measurements.

The model of rigid micro-blocks estimates the character of deformations between the Aragats and Vardenis micro-blocks as extension at a rate of 3.1 ± 0.8 mm/yr with the azimuth of 69.7° (Fig.5). If the fixed point approach is followed, the analysis of velocity vectors for stations

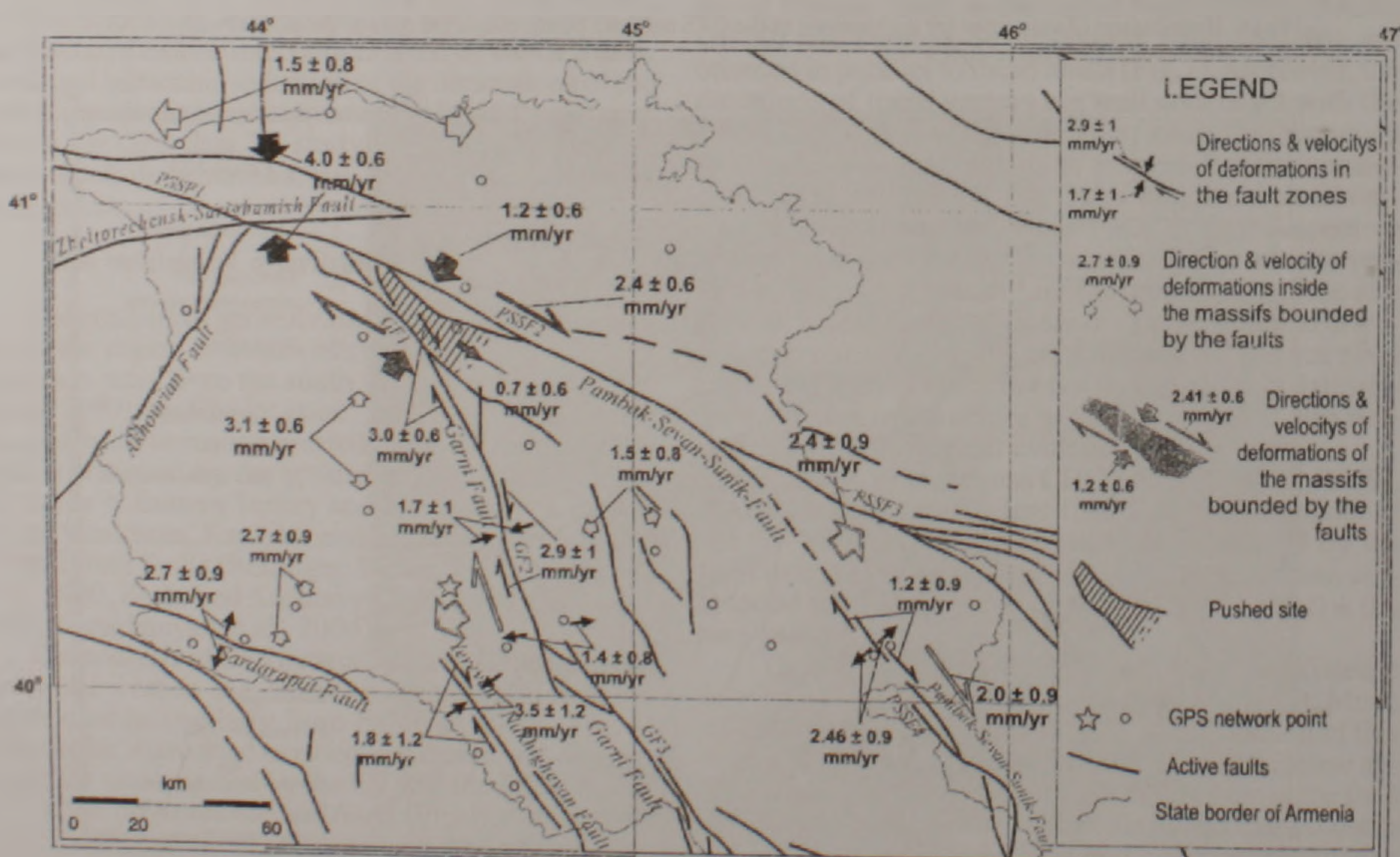


Fig.8: Estimated deformation rates and directions in fault zones and intra-fault areas across central and northern Armenia

Table 7

Comparison of the active fault slip rates derived by long-term and short-term geological evidence, and also by the data of GPS observations

| Fault | Faults segment | Geological Data Long-term Slip Rate | | Geological Data Short-term Slip Rate | | GPS Data | |
|--------------------------|----------------------------|----------------------------------------|-------------------------------------------------------------------------------------------|-----------------------------------------|-------------------------------------------|--------------------------------|--------------------|
| | | Motion Component | Rate | Motion Component | Rate | Motion Component | Rate |
| Pambak-Sevan-Sunik Fault | PSSF 2 Vanazor-Artanish | Strike-Slip (right-lateral) | 3-4 mm/yr (Trifonov et al. 1990) 2.24 ± 1 mm/yr (Philip et al. 2001) | - | - | - | - |
| | PSSF 3 Artanish-Tskhuk | Strike-Slip (right-lateral) | 3-4 mm/yr (Trifonov et al. 1994) 0.53 -0.64 mm/yr (Philip et al. 2001) | Strike-Slip (right-lateral) | 0.64 ± 0.07 mm/yr (Philip et al. 2001) | Strike-Slip (right-lateral) | 1.2 ± 0.9 mm/yr |
| Garni Fault | GF1 Alavar-Lernapat | Strike-Slip (right-lateral) | 3 ± 0.5 mm/yr (Trifonov et al. 1994) | - | - | Strike-Slip (right-lateral) | 3.0 ± 0.6 mm/yr |
| | GF2 | - | - | - | - | Strike-slip (right-lateral) | 2.9 ± 1 mm/yr |
| | GF3 | - | - | - | - | Shortening | 1.7 ± 1 mm/yr |
| Yerevan-Nakhigevan Fault | YNF1 | - | - | - | - | Extension | 1.4 ± 0.8 mm/yr |
| | - | - | - | - | - | Strike-Slip (right-lateral) | 1.8 ± 1.2 mm/yr |
| Sardarapat Fault | - | - | - | - | - | Shortening | 3.5 ± 1.2 mm/yr |
| | - | - | - | - | - | Extension | 2.7 ± 0.9 mm/yr |

and ZOD0 indicates that this deformation can be assessed as extension at a rate of 2.4 ± 0.9 mm/y with the azimuth of 58° and right-lateral motion at 2.0 ± 0.9 mm/y (Fig.8). Along with this, extensive deformation between these stations increases regularly in the eastward direction (Fig.6a). By analyzing the velocities of stations RAZ0, GEG0, SHA0 and TSA0, it was possible to estimate the inner deformation for the area delimited by the GF and the PSSF, which accommodates several active faults and is characterized by 1.5 ± 0.8 mm/y of extension with the azimuth of 64° (Fig.8). The difference of deformation velocity vectors measured at stations CHO0, ODZ0, PAM0 and ENO0 has determined the sense and the rate of deformation between CHO0 and the Tavoush site, where a right-lateral strike-slip with a shortening component is recorded. The strike-slip motion has a rate of 2.4 ± 0.6 mm/y, and the shortening has a rate of 1.2 ± 0.6 mm/y (Fig.8). The analysis of measurements at CHO0, SHA0 and PAM0 suggests that a triangular

wedge, outlined by the Vanadzor-Artanish segment of the PSSF and the Alavar segment of the GF, with the tip located at the crossing between the PSSF and the GF, is pushed to the southeast.

This site is marked with hatching in Figure 8. The site is pushed at an estimated rate of 0.7 ± 0.6 mm/y (Fig.8).

Discussion and Conclusions

The analysis presented above casts doubts upon the assumed existence of rigid, non-deformed micro-blocks in central and northern Armenia, with the Holocene-recent tectonic activity.

The model of rigid micro-blocks can be used only to give a generalized regional characteristic of deformation for large regions of the Southern and Northern Caucasus, Eastern Anatolia and Western Iran relative to the Eurasian continental plate. From the standpoint of such characteristic, the northern drift of the Aragats The

kinematics of the northern YNF segment is NSSP micro-block provokes squeezing of the micro-blocks on its eastern boundary out in the north-eastern direction and causes compressive deformation near the apex of the North-Armenian tectonic arc. This pattern derived by the GPS data confirms the geological evidence (Trifonov et al., 1994; Karakhanyan, 1995; Karakhanyan et al., 2004)

The model of distributed deformation produces a remarkable picture of deformation distribution inside the Aragats massif bounded by the Garni Fault and the Akhouryan Fault, with alternation of extension and compression zones oriented north-to-south (Fig.6c). The result is that against the background of general shortening of the Earth crust recorded by the global GPS network in the N-S direction (Reilinger et al., 1996), the local GPS network in Armenia registers extension areas oriented in the same N-S direction. Aragats stratovolcano is situated in the central part of the area of alternating compression and extension in the N-S direction. The velocities measured by GPS stations on the southern slopes of the Aragats volcano and to the south of it (SA20, SA10, MET0, BUR0) are considerably less than the velocities of station CHO0, located north of Aragats (Fig.4). This implies that with the general attenuation of deformation rates from the south to the north in the central part of the Arabian collision (Reilinger, 1997, McClusky et al., 2000), a reversed pattern of increasing velocities is observed for the Aragats Volcano site. Most probably, this is related to some internal local deformations inside the massif of Aragats Volcano, the character of which has not been yet understood.

The use of the method of fixed GPS station allows us to estimate slip rates for the main active faults in Armenia. Table 7 shows that deformation estimate for the GF1 segment of the Garni Fault (right-lateral strike-slip of $3.0 \pm 0.6 \text{ mm/yr}$) is consistent with the geological estimate derived by the displacement of morphological elements. The GPS-derived rate of deformation for the zone of the GF2 segment of the Garni Fault (the right-lateral displacement at $2.9 \pm 1 \text{ mm/yr}$ with the shortening component of $1.7 \pm 1 \text{ mm/yr}$ (Fig.8)) is strong evidence in favor of the existence of GF2.

The southern flank of GF2 joins the GF3 segment forming a structure of Pull Apart Basin. Karakhanyan et al. (2004) supposed that the source of the 1679 Garni earthquake with $M = 6.9$ was located in this zone. In the same area, we have recorded extensive deformation at the rate of $1.4 \pm 0.8 \text{ mm/yr}$ (Fig.8) (Table 7).

For the Pambak-Sevan-Syunik Fault, the comparison of displacement rates derived by geological evidence and by the GPS measurements could be made only for its Artanish-Tskhouk segment (Table 7), but the inconsistencies are here noticeable. The estimates of long-term displacement rate by the geological evidence are varying from 3.4 mm/yr according to Trifonov et al. (1994) to $0.53\text{-}0.64 \text{ mm/yr}$ according to Philip et al. (2001). The GPS-derived deformation rate value (right-lateral strike-slip of $1.2 \pm 0.9 \text{ mm/yr}$ and extension of $2.5 \pm 0.9 \text{ mm/yr}$) is not correlating either with the long-term or short-term geological estimates. The long-term assessment of slip rates was based on the measured offsets of morphology elements. Therefore, the resulting value depends on the accuracy of displacement measurement, and of the age and date of the considered morphology element offset. The Khonarassar Volcano cut by the fault and dislocated by 750 meters served as

such element for the long-term assessment of the Artanish-Tskhouk segment (Trifonov et al., 1994; Philip et al. 2001). The accuracy of dislocation measurement and, primarily, of the age estimated for the dislocated volcano influenced the final estimation of the slip rate by the geological data.

There is no doubt that the differences between the values obtained by geological and geodetic methods for slip rates along active faults can reflect changes of these rates through the elapsed geological time. One can expect that recent estimates derived by GPS measurements will be inconsistent with the averaged rates estimated by long-term geological evidence, while the latter will be in conflict with the short-term geological estimates, since except of pulsed co-seismic motions there are also slower creep motions to take into account.

The outcome of the studies performed indicates that use of dense GPS network can be highly efficient for resolving geodynamic problems at a detailed level and estimating slip-rates for individual fault zones. The obtained results can be used both for the analysis of geodynamics in Armenia and Southern Caucasus, and for seismic hazard assessment in Armenia. In the meantime, it should be noted that to make full analysis of the velocities and deformation fields over the entire territory of Armenia, our GPS network should be extended in the southern direction. This must allow measurement of GPS velocities for the southern continuation of the Pambak-Sevan-Syunik Fault and the Garni Fault. The GPS methods still have not been applied to measure rates of deformations for the Akhouryan and Zheltorechensk-Sarighamish that are the left-lateral strike-slip faults. Parts of these faults spread into Turkey and Iran, and this substantiates the need for joint international GPS studies in the region.

Acknowledgements

This study would not be possible without the well-coordinated work of a large French-Armenian team. We express our gratitude to all participants of the GPS sessions conducted from 1997 to 2003 (Abelyan M., Arakelyan S., Bagdasaryan G., Bagdasaryan H., Bayer R., Calais, E., Chery J., Collard, P., Daigniere, M., Gasparyan M., Gerbault, F., Harnard, E., Harutunyan R., Khachinjan V., Masson, M., Mkrtchyan A., Mkrtchyan S., Peyret, M., Ritz, J.F., Sargissyan S., Vernant, P.).

We are grateful also to Dr. V. Trifonov (Institute of Geology, Russian Academy of Sciences) for his continuous and important help and participation in the course of GPS surveys and other studies in Armenia. We thank Prof. R. Jrashyan, Academician of the National Academy of Sciences of Armenia, for his valuable assistance in the organization and implementation of the GPS studies in Armenia. Our GPS investigation in Armenia was made possible thanks to the financial support of the PICS Project on *Creation of GPS networks in Armenia: Monitoring of Geodynamics* and of the *Fonds Armenien de France* represented by Mr. Karpis Jrashyan. We want to thank the population of the villages of Geghakar, Akhburazor, Pambak and other communities in Armenia who helped us in the organization of field surveys. We appreciate the invaluable help of V. Trifonov and Y. Abgaryan in the preparation of this article. We believe that all participants of the GPS surveys are the co-authors of this work.

REFERENCES

- Altamimi Z., P. Sillard, and C. Boucher.** ITRF2000. A new release of the International Terrestrial Reference Frame for earth sciences applications, *J. Geophys. Res.*, 2002, 107 (B10), NIL-119-NIL-137.
- Ambraseys N.N., Jackson J.A.** Faulting associated with historical and recent earthquakes in the Eastern Mediterranean region. *Geophys. J. Int.* 1998, 133, 390–406.
- Ambraseys N.N., Melville C.P.** A History of Persian Earthquakes. New York, Cambridge Univ. Press. 1982, p. 219.
- Avagyan A.** Estimation of slip rates and recurrence intervals of strong earthquakes on the fault system of Pambak-Sevan-Sunik (Armenia): segmentation and relation with volcanic activity. PhD Thesis, Montpellier II University, France, 2001, 180 p.
- Avagyan A., Sosson M., Philip H., Karakhanian A., Rolland Y., Melkonyan R., Rebai S., and Davtyan V.** Neogene to Quaternary stress field evolution in Lesser Caucasus and adjacent regions using fault kinematics and volcanic cluster data. *Geodinamica Acta*. (In press 2006).
- Balassanian S. Y., Nazaretsian S. N., Avanessian A. S., Arakelian A. R., Igumnov V. A., Basalian M., Martirosyan A. H., Ambartsumian V., and Tovmassian A. K.** The new seismic zonation map for the territory of Armenia, *Natural Hazards* 15, 231–249. 1997.
- Balassanian S., Melkoumian M., Arakelyan A., and Azarian A.** Seismic Risk Assessment for the Territory of Armenia and Strategy of its Mitigation, *Natural Hazards* 1999a, 20, 43–55. Kluwer Academic Publishers
- Balassanian S., Martirosyan A., Simonian R., Asatryan L.** "Computation of Probabilistic Seismic Hazard for the GSHAP Test Area "Caucasus". *Natural Hazards* 1999b, 20: 1-20. Kluwer Academic Publishers
- Balassanian S., Avanessian A., Akopyan G., and Reilinger R.** GPS-Observation on the Armenia Territory, *Earthquake Engineering*, 1999c, N1, p.32.
- Barka A.A., Kadinsky-Cade K.** Strike-slip fault geometry in Turkey and its influence on earthquake activity. *Tectonics*, 1988, 3, pp. 663–684.
- Barka A. and R. Reilinger.** Active tectonics of the Eastern Mediterranean region: derived from GPS, neotectonic and seismicity data, *Annali di Geofisica*, 1997, XL (3), pp. 587–610
- Berberian M.** Seismic sources of the Transcaucasian historical earthquakes. In: Giardini, D., Balassanian, S. (Eds.), Historical and Prehistorical Earthquakes in the Caucasus. Kluwer Academic Publishing, Dordrecht, Netherlands. 1997, pp. 233–311
- De Mets C., Codon R.G., Argus D.F., and Stein S.** Current plate motion. *Geophys. J. Int.*, 1990, 101, pp. 425–478
- Dewey J. F., Hempton M.R., Kidd W.S.F., Saroglu F., and Sengor A.M.C.** Shortening of continental lithosphere: the neotectonics of Eastern Anatolia—a young collision zone. In: Coward, M.P., Rica, A.C. (Eds.), Collision Tectonics. *Geol. Soc. Lond. Spec. Publ.*, 1986, vol. 19, pp. 3–36.
- Doerslinger E., Masson F., Bayer R., Avagyan A., Philip H., Ritz J.-F., Daignieres M., Gerbault M., Peyret M., Collard P., Karakhanian A., Aslanian R., Jerbashian R., Calais E.** The Present Strainfield in Lesser Caucasus: Setting of a GPS Network in Armenia, (Poster) European Union of Geosciences (EUG 99). 1999, Strasbourg, France, April.
- Guseva T., Skvorodkin Yu.** Post-seismic deformation of the Spitak fault using distance measurements data. The Second International Conference on Earthquake Hazard and Seismic Risk Reduction. The International Decade for Natural Disaster Reduction (IDNDR). Regional Conference for the Countries of the Commonwealth of Independent States (CIS) and Eastern Europe. 1998, Yerevan, Armenia, p.109.
- Herring T.A.** Documentation for the GLOBK software version 9.5. Massachusetts Institute of Technology, Cambridge, MA. 2001
- Jackson J.A. & McKenzie D.P.** Active tectonics of the Alpine-Himalayan belt between western Turkey and Pakistan, *Geophys. J. R. astr. Soc.*, 1984, 77, pp. 185–264.
- Karakhanian A., Trifonov V.G., Azizbekian O.G., Honkarian D.G.** Relationship of the late Quaternary tectonics and volcanism in the Khonarassar active fault zone, the Armenian Upland. *Terra Nova*, 1997a, 9, pp. 131–134
- Karakhanian A., Djrbashyan R.T., Trifonov V.G., Philip H., and Ritz J.F.** Active faults and strong earthquakes of the Armenian Upland. In: Giardini, D., Balassanian, S. (Eds.), Historical and Prehistorical Earthquakes in the Caucasus. Kluwer Academic Publishing, Dordrecht, Netherlands, 1997b, pp. 181–187
- Karakhanian A., Trifonov V., Philip H., Avagyan A., Hessami K., Jamali F., Bayraktutan M. S., Bagdassarian H., Arakelian S., Davtian V., and Adilkhanian A.** Active faulting and natural hazards in Armenia, eastern Turkey and north-western Iran. *Tectonophysics*, 2004, 380, pp. 189–219
- King R., Bock Y.** Documentation for the GAMIT GPS software analysis version 10.05, Massachusetts Institute of Technology, Cambridge, MA. 2001
- McClusky S., S.Balassanian, A.Barka, C.Demir, S.Ergintav, I.Georgiev, O.Gurkan, M. Hamburger, K.Hurst, H.Kable, K.Kasten, G.Kekelidze, R.W.King, V.Kotzev, O.Lenk, S.Mahmoud, A.Mishin, M.Nadariya, A.Oezoumis, D.Paradissis, Y.Peter, M.Prilepin, R.Reilinger, I.Sauli, H.Seeger, A.Tealeb, M.N.Toksöz, and G.Veis.** GPS constraints on plate motions and deformations in eastern Mediterranean and Caucasus, *J. Geophys. Res.* 2000, 105, pp. 5695–5719.
- Philip H., Avagyan A., Karakhanian A., Ritz J.-F., and Rebai S.** Slip rates and recurrence intervals of strong earthquakes along the Pambak-Sevan-Sunik fault (Armenia). *Tectonophysics* 343 (3–4), 205–232. 2001
- Rebai S., Philip H., Dorbath L., Berissoff B., Haessler H., and Cisternas A.** Active tectonics in the Lesser Caucasus coexistence of compressive and extensional structures. *Tectonics*, 1993, 12, 5, pp. 1089–1114
- Reilinger R., McClusky S., Souter B., Hamburger M., Mishin A., Guseva T., and Balassanian S.** Global Positioning System measurements of plate convergence in the Caucasus continental collision zone, *J. Geophys.* 1996.
- Reilinger R., Barka A.** GPS constraints on fault slip rates in the Arabia-Africa-Eurasia plate collision zone: implications for earthquake recurrence times. In: Giardini, D., Balassanian, S. (Eds.), Historical and Prehistorical Earthquakes in the Caucasus, ILP publication 333, NATO ASI Series 28. Kluwer Academic, Dordrecht, 1997, pp. 91–108.
- Taymaz T., Eyidogan H., and Jackson J.** Source parameters of large earthquakes in the East Anatolian fault zone (Turkey). *Geophys. J. Int.*, 1991, 106, pp. 537–550.
- Trifonov V.G., Karakhanian A.S., Kozhurin A.I.** The Spitak earthquake as a manifestation of active tectonics. *Geotektonika* 6, 1990, 46–60 (in Russian)
- Trifonov V., Karakhanian A., Kozhurin A.** Major active faults of the collision area between the Arabian and the Eurasian plates. Proc. of the Conference on Continental Collision Zone Earthquakes and Seismic Hazard Reduction. IASPEI/IDNDR, Yerevan, 1994, pp. 56–79.
- Караханян А.** Активные разломы и сильные землетрясения Ангтолийско-Кавказского региона. Диссертация на соискание ученой степени доктора геологических наук. Москва, ИФЗ, 1995, 298 с.
- Шевченко В. И., Гусева Т. В., Лукк А. А. и др.** Современная геодинамика Кавказа по результатам GPS измерений и сейсмологическим данным. *Физика Земли*, 1999 (9) С.3–18

ԽԶՎԱԾՔՆԵՐԻ ՏԵՂԱԾԱՐԺԻ ԱՐԱԳՈՒԹՅՈՒՆՆԵՐԸ ՀԱՅԱՍՏԱՆՈՒՄ Ըստ GPS ՏՎՅԱԼՆԵՐԻ

Վ. Դավթյան, Է. Դորֆլինցեր, Ա. Կարախանյան, Է. Ֆիլիպ,
Ա. Ավազյան, Ս. Շամպուլյոն, Ռ. Աղանյան

Ա մ փ ո փ ո ւ մ

Հայաստանի Հանրապետության տարածքում գերակշռում են կարճ կողաշարժային բնույթի ակտիվ խզվածքները, որոնք ունեն վերնետքային և վարներքային ուղղահայաց բաղադրիչներ (Trifonov et al., 1994; Philip et al., 2001; Karakhanyan et al., 1997a, 1997b, 2004; Anagyan, 2001): Այդ խզվածքների երկարությունը չի անցնում 350-450 կմ-ը, սակայն նրանց հետ կապված երկրաշարժերը ունեն $M = 7.2 - 7.5$ սագնիտուդներ (Ambraseys and Melville, 1982, Berberian, 1997, Karakhanian et al., 2004): Երկրադինամիկան և սեյսմիկ ակտիվության դրսերումները այստեղ բարդ են և քիչ ուսումնասիրված: Ըստ խզվածքների տեղաշարժի արագությունների, առավելագույն հնարավոր մագնիտուդների և երկրաշարժերի կրկնողության պարբերությունների գնահատականները մասնակի են և անհասկանալի:

Սկսած 1998թ-ից Մոնպելի-2 (Ֆրանսիա) համալսարանի, “Գեոդիսկ” ընկերության (Հայաստան) և ՀՀ ԳԱԱ Երկրաբանական գիտությունների ինստիտուտի (Հայաստան) կողմից սկսվել են համաստեղ GPS հետազոտություններ ակտիվ խզվածքների գոտիներում՝ դեֆորմացիաների հետազոտման նպատակով:

Այդ իսկ պատճառով, ի լրացում MGN ցանցին (Mediterranean GPS Network) ՀՀ կենտրոնական և հյուսիսային հատվածներում տեղադրվել է GPS ցանց, որը բաղկացած է 22 կետերից (Doerflinger et al., 1999): Ստեղծված ցանցը ծածկում է ՀՀ հյուսիսային և կենտրոնական հատվածների առավել ակտիվ և երկրադինամիկայի տեսակետից հնտաքրքիր գոտիները, սրոնք ունեն սեյսմիկ ոիսկի առավելագույն մակարդակ: Ցանցը հյուսիսային լայնությամբ տարածվում է 150 կմ, իսկ արևելյան երկայնությամբ՝ 180կմ:

GPS դիտարկումները իրականացվել են 1998, 2000 և 2003 թվականներին: Չափումներում օգտագործվել են Ashtech Z12 և Ashtech ZX տիպի երկհաճախականային փուլային GPS ընդունիչներ, որոնք հագեցած են Ashtech Chock Ring տիպի ալեհավաքներով:

Ցանցի կետերի կոռորդնատների և նրանց տեղաշարժի արագությունների հաշվարկներն իրականացվել են GAMIT 10.05 (King and Bock, 2001) և GLOBK 10.0 (Herring, 2001) ծրագրային փաթեթների միջոցով: Կետերի տեղադիրքի և արագությունների որոշումը կատարվել է ITRF2000 համակարգում:

Ստացված դեֆորմացիաների արագությունների վերլուծությունը բույլ է տալիս հերքել այն կարծիքը, որը վերաբերվում է լիբոսֆերայի կոչու շվեֆորմացված բլոկների գոյությանը (Balasanyan et al., 1999 a,b) ՀՀ կենտրոնական և հյուսիսային հատվածներում: Ինչ վերաբերվում է նվազագույն մայրցամաքային սալի նկատմամբ Հարավկովկասյան տարածաշրջանի խոշոր զանգվածների դեֆորմացիաների ընդհանրացված բնութագրերին, ապա կարելի է նշել, որ Արագածի զանգվածի հյուսիսային որեյֆը, որը սահմանափակված է Գառնիի և Ախուրյանի խզվածքներով, հարուցում է նրա հետ արևելքից սահմանակցող զանգվածի դուրս մղում հյուսիս-արևելյան ստղությամբ, որն էլ իր հերթին հանգեցնում է Հյուսիսական տեկտոնական սուրբության բարձրացույթի հատվածի սեղմման դեֆորմացիայի: GPS տվյալներով ստացված պատկերը հաստատում է (Trifonov et al., 1994; Karakhanyan, 1995; Karakhanian et al., 2004) երկրաբանական տվյալները:

Հետաքրքիր տեսարան է նկատվում Արագածի զանգվածի ներսում: Այստեղ արծանագրվում են Հյուսիս-Հարավ ուղղվածությամբ ընդարձակնան գոտիներ: Այսինքն Կովկասի երկրակեղերի Հյուսիս-Հարավ կրծատման ընդհանուր ֆոնի վրա (Reilinger et al., 1996) կան ընդհարձակնան գոտիներ միևնույն ուղղությամբ: Այն GPS կայանների արագությունները Եվրասիայի նկատմամբ, որոնք գտնվում են Արագած իրարուխի հարավային լանջերին և ավելի հարավ (SA20, SA10, MET0, BUR0), էապես փոքր են, քան այն կայաններինը, որոնք տեղադրված են Արագածից հյուսիս (CHO0): Այսինքն, ի տարբերություն Եվրասիական և Արաբական սալերի բախման կենտրոնական հատվածում դեֆորմացիաների արագությունների Հյուսիս-Հարավ ուղղվածության մարման տեսնենցին, նկարագրվող տեղամասում մենք նկատում ենք հակառակը: Հավանական է, որ պայ-

մանավորված է Արագածի հրաբխային զանգվածի սեփական, ներքին դեֆորմացիաներով. որոնք արագացումներ են հաղորդում առավել հյուսիսային կետերին:

Անցկացված GPS հետազոտությունները թույլ տվեցին գնահատել խզվածքային գոտիների դեֆորմացիաների արագությունները, մասնակի դեպքերում նաև ըստ սեզմենտների, ՀՀ կենտրոնական և հյուսիսային հատվածներում: Գառնիի խզվածքի GF1 սեզմենտում դեֆորմացիաները գնահատվել են որպես աջակողմյան կողաշարժեր տարեկան 3.0 ± 0.6 մմ/տարի արագությամբ: GF2 սեզմենտի կինեմատիկան բնութագրվում է որպես աջակողմյան կողաշարժ սեղմումով, ընդ որում կողաշարժի արագությունը կազմում է 2.9 ± 1 մմ/տարի: իսկ սեղմման արագությունը 1.7 ± 1 մմ/տարի:

Փամբակ-Սևան-Սյունիք խզվածքի Արտանիշ-Ծխուկի սեզմենտը ըստ GPS տվյալների գնահատված է որպես աջակողմյան կողաշարժ սեղմման բաղադրիչով: Կողաշարժի արագությունը կազմում է 1.2 ± 0.9 մմ/տարի, իսկ ընդարձակման արագությունը կազմում է 2.5 ± 0.9 մմ/տարի:

Երևան-Նախիջևան խզվածքի հյուսիսային սեզմենտի կինեմատիկան գնահատվել է KHO0 և KAR0 կայաններով, որպես աջակողմյան կողաշարժ սեղմման բաղադրիչով, որտեղ գերակշռում է սեղմման դեֆորմացիան 3.5 ± 1.2 մմ/տարի արագությամբ, միևնույն ժամանակ կողաշարժի արագությունը կազմում է 1.8 ± 1.2 մմ/տարի: Սարդարապատի խզվածքի գոտում գրանցվել է ընդարձակում 2.7 ± 0.9 մմ/տարի արագությամբ:

Հյուսիսայիկական տեկտոնական աղեղի կենտրոնական հատվածում արծանագրվել է սեղմում Հյուսիս-Հարավ ուղղվածությամբ, 4.0 ± 0.6 մմ/տարի արագությամբ:

СКОРОСТИ СМЕЩЕНИЯ ПО РАЗЛОМАМ В АРМЕНИИ ПО ДАННЫМ GPS

В. Давтян, Э. Доэрфлинджер, А. Караканян,
Э. Филип, А. Авагян, С. Шамполлион, Р. Асланян

Резюме

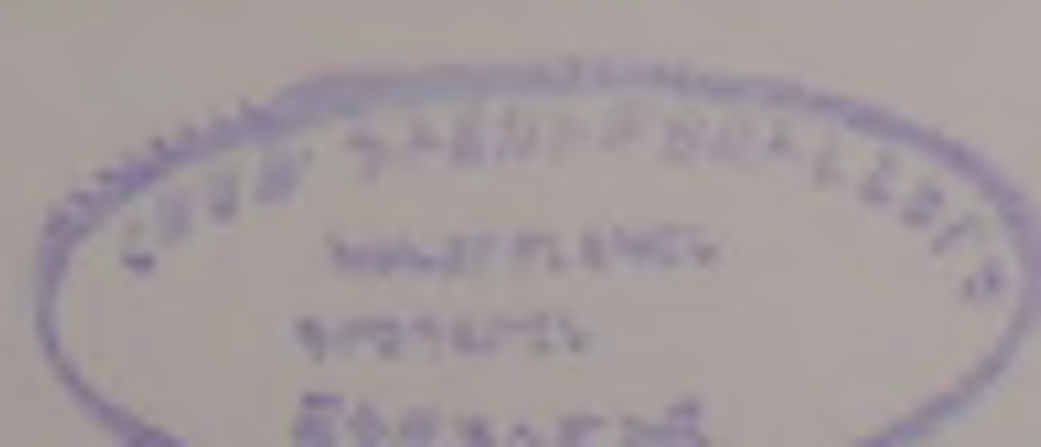
На территории Армении преобладают активные сдвиговые разломы с взбросовой, или сбросовой вертикальной компонентой (Trifonov et al., 1994; Philip et al., 2001; Karakhanian et al., 1997a, 1997b, 2004; Avagyan, 2001). По длине эти разломы не превышают 350 – 450 км, однако с ними связаны землетрясения с $M=7.2-7.5$ (Ambraseys, Melville, 1982; Beberian, 1997; Karakhanian et al., 2004). Проявления геодинамической и сейсмической активности здесь сложны и изучены недостаточно. Оценки скоростей смещений по разломам, а также максимально возможных магнитуд и периодов повторяемости землетрясений отрывочные и неясны.

Начиная с 1998 года, университетом Монпелье-2 (Франция), компанией "Геориск" и Институтом геологии НАН РА (Армения) были начаты GPS исследования по изучению деформаций в зонах активных разломов. Для этого, в дополнение к сети MGN (Mediterranean GPS Network), в центральной и северной частях территории Армении была установлена GPS сеть из 22 точек (Doerflinger et al., 1999). Созданная сеть покрывала наиболее активные и геодинамически интересные области на севере и в центре Армении, с максимальным уровнем сейсмического риска. Протяженность сети составляет 150 км по широте и 180 км по долготе.

Сессии измерений в сети GPS были проведены в 1998, 2000 и в 2003 годах. Измерения проводились двухчастотными фазовыми GPS приемниками Ashtech Z12 и Ashtech ZX, оснащенными антеннами Ashtech типа Chock Ring.

Определение координат точек сети и скоростей их движения было выполнено в системе ITRF2000 с помощью программных пакетов GAMIT 10.05 (King and Bock, 2001) и GLOBK10.0 (Herring, 2001).

Анализ полученных скоростей деформаций позволяет опровергнуть допущение о существовании жестких недеформируемых блоков литосферы (Balasanyan et al., 1999a,b) на территории центральной и северной Армении. С точки зрения обобщенной характеристики деформаций крупных регионов Южного Кавказа относительно Евразийской континентальной плиты, можно отметить, что северный дрейф Арагацкого массива, ограниченного Гарнийским и Ахурянским разломами, провоцирует выталкивание в северо-восточном направлении граничащих с ним с востока участков и вызывает деформацию сжатия в области вершины Североармянской тектонической



дуги. Подобная картина, полученная по GPS данным, подтверждает геологические данные (TGFonow et. al., 1994; Караканян, 1995; Karakhanian et. al., 2004).

Интересная картина наблюдается внутри Арагацкого массива. Здесь фиксируются зоны растяжения, ориентированные в направлении С-Ю. То есть, на фоне общего укорочения коры Кавказа в направлении С-Ю (Reilinger et al., 1996) имеются области растяжения, ориентированные в том же направлении. Скорости GPS станций, находящихся на южных склонах вулкана Арагац и южнее (SA20, SA10, METO, BURO), относительно Евразии, существенно меньше, чем скорость станции CHOO, находящейся севернее Арагаца. Таким образом, вопреки тенденции затухания скоростей деформаций в центральной части Аравийско-Евразийской континентальной коллизии с Юга на Север, на описываемом нами участке, мы наблюдаем обратное. Вероятнее всего это связано с собственными, внутренними деформациями массива вулкана Арагац, которые и придают ускорение более северной точке.

Проведенные GPS исследования позволили оценить скорости деформаций в зонах разломов, а иногда и их сегментов, центральной и северной Армении. Деформация в зоне сегмента Гарнийского разлома GF1 оценена как правый сдвиг со скоростью 3.0 ± 0.6 мм/год. Кинематика сегмента GF2 – как правосторонний сдвиг со сжатием, причем скорость сдвига составила 2.9 ± 1 мм/год, а скорость сжатия – 1.7 ± 1 мм/год.

Кинематика Артаниш-Цхукского сегмента Памбак-Севан-Сюникского разлома, по данным GPS, оценена как правосторонний сдвиг с растяжением. Скорость сдвига составляет 1.2 ± 0.9 мм/год, скорость растяжения – 2.5 ± 0.9 мм/год.

Кинематика северного сегмента Ереван-Нахичеванского разлома оценивается по станциям KHOО и KARO как правосторонний сдвиг с компонентой сжатия, при том что доминирует сжатие, скорость которого составляет 3.5 ± 1.2 мм/год, а скорость сдвига составляет 1.8 ± 1.2 мм/год. В зоне Сардарапатского разлома зафиксировано растяжение со скоростью 2.7 ± 0.9 мм/год.

В области центральной части Североармянской тектонической дуги зафиксировано сжатие в направлении Ю-С со скоростью 4 ± 0.6 мм/год.